SSRG International Journal of Civil Engineering
ISSN: 2348-8352/ https://doi.org/10.14445/23488352/IJCE-V10I9P104

Volume 10 Issue 9, 29-43, September 2023

Original Article

Seismic Vulnerability Assessment of Steel Moment Resisting Frame Equipped with Friction Damper

Swapnil B. Kharmale[1], Chetan S. Patil[2], Veeranagouda B. Patil[3]

[1]*Civil Engineering Department, Government College of Engineering and Research, Avasari (Kd), Maharashtra, India.*
[2]*Civil Engineering Department, Sanjay Ghodawat University, Kolhapur, Maharashtra, India.*
[3]*Civil Engineering Department, KLE Technological University, Hubballi, Karnataka, India.*

[1]*Corresponding Author : sbkharmale.civil@gcoeara.ac.in*

Received: 13 July 2023 Revised: 27 August 2023 Accepted: 15 September 2023 Published: 30 September 2023

Abstract *- This research evaluates the likelihood of seismic collapse for high-rise Steel Moment Resisting Frames (SMRF) designed with a recently developed Performance-Based Plastic Design (PBPD) approach and equipped with friction dampers. A 21-storey SMRF designed according to the PBPD method for three different displacement ductility ratios is equipped with supplementary friction dampers to overcome largely concentrated and non-uniformly distributed inter-storey drifts at higher storeys. Multi-record Incremental Dynamic Analysis (MIDA) of three different ductility designs of SMRF with and without supplementary friction dampers is performed under the suite of selected vital motion records. The seismic fragility of these PBPD designs of SMRF with and without additional friction damper is used to identify the optimum range of the seismic hazards to minimize the total likelihood of damages under solid ground motion. Results show that friction dampers are highly effective in reducing the probability of high-rise SMRF seismic collapse designed with the PBPD approach.*

Keywords *- Steel Moment Resisting Frames (SMRF), Performance-Based Plastic Design (PBPD), Multi-record Incremental Dynamic Analysis (MIDA), Friction damper, Seismic fragility.*

1. Introduction

For high to medium seismic regions around the globe, the Steel Moment Resisting Frame (SMRF) is still the most extensively used Lateral Load Resisting System (LLRS). Structural failures demonstrated the weaknesses of the general design and construction procedures of such SMRFs noted after the 1994 Northridge and 1995 Kobe earthquakes [1-2]. Advanced design approaches and performance assessment techniques were subsequently developed after these two events. A Performance-Based Plastic Design (PBPD) method for various LLRS using target inelastic drift and preselected yield mechanism based on the uniform inter-storey drift was developed at the University of Michigan [3-5].

This method uses the concept of energy balance displacement ductility ratio (μ_s) in calculating seismic design base shear (V_{by}); however, it explicitly does not account for P-Delta and higher mode effects. Thus, medium to high-rise SMRFs designed with the PBPD approach exhibit non-uniform, primarily concentrated residual inter-storey drifts for moderate to high ductility demands under strong earthquakes [5-6]. Various passive energy dissipation devices have been extensively studied to prevent or reduce seismic damage from the central structural systems [7, 8]. To dissipate seismic energy and reduce plastic deformations in the structural elements, passive dissipation devices use friction mechanisms or the mechanical properties of some materials, such as rubber, steel, lead, viscous and visco-elastic materials. Single diagonal tension/compression braces with sliding friction damper, as proposed by Pall and Marsh [9], are considered one of the most efficient and widely used passive devices for reducing the structural damage caused by earthquakes.

The essential advantage of these friction dampers is large rectangular hysteresis loops offering greater energy dissipation without any sophisticated installation techniques. Thus, friction dampers act as displacement reducers for serviceability requirements and energy dissipators under severe seismic actions [10-12]. The initial application of supplementary friction damper was for seismic retrofitting of steel and reinforced concrete moment resisting frame [13, 14]. Experimental and numerical research on friction dampers to investigate their energy-dissipating capacity and formulate their design procedure can be traced in the literature [15-20]. The actual life application of Pall Friction Damper (PFD) in various modern commercial buildings across the globe proved its practicality and efficient performance [21].

1.1. Motives for the Research

In the context of past research [11–21], supplementary damping devices (passive and active dampers) are explored for structural systems designed by force/strength-based approach, where these dampers are meant to meet the serviceability requirements of design standards. The need and applications of such supplementary damping devices in structural systems designed using a recently developed PBPD framework have not been investigated yet. Higher mode and P-Delta effects, largely concentrated and non-uniform inter-storey drifts under severe strong motion, are often significant for flexible SMRF designed with the PBPD method. In such a design scenario, using supplementary friction dampers to control the inelastic drift and dissipate inelastic energy demand under strong motion can be considered an efficient approach. Thus, the research presented here mainly focuses on ascertaining the use of supplementary energy-dissipating devices in PBPD designs and justifies their application through seismic collapse assessment study.

1.2. Objectives and Outline of Study

The primary thrust of work presented after this is: a) to use friction dampers as supplementary energy dissipating devices in PBPD designs of 21-storey SMRF for moderate to high displacement ductility demands to overcome P-Delta effect as well as primarily concentrated and non-uniform inter-storey drifts, b) to assess seismic collapse vulnerability of PBPD designs of SMRF with and without supplementary friction dampers through nonlinear Multi-record Incremental Dynamic Analysis (MIDA), and c) to compare the probability of collapse of 21-storey SMRF equipped with various configurations of friction dampers for a given displacement ductility ratio.

Considering the objectives of the present study, the recently developed PBPD method [3] and its application to the design of a 21-storey SMRF for three different levels of displacement ductility ratios are discussed in the subsequent section. Section 3 deals with analytical testing of PBPD of 21-storey SMRF using Nonlinear Static Pushover Analysis (NSPA), Nonlinear Time History Analysis (NTHA), and supplementary friction dampers in these designs. The seismic fragility of PBPD designs of SMRF with and without supplemental friction dampers through nonlinear Multi-record Incremental Dynamic Analysis (MIDA) under the suite of 20 ground motion records of extensive Magnitude Short Range (LMSR) is presented in Section 4. The findings, conclusions, present study, and scope for future research are summarized in the last section.

2. Performance-Based Plastic Design Method with Design of 21-storey SMRF

Energy balance [3, 22] and plastic design formulation are used in the recently developed Performance-Based Plastic Design (PBPD) method. The effectiveness of PBPD philosophy is ascertained for steel braced frames [4], reinforced concrete special moment resisting frames [23], and tall hybrid coupled walls [24], where this method proved to be very efficient in achieving preselected performance objectives in terms of yield mechanism and target drift.

2.1. PBPD Method by Lee and Goel [3]

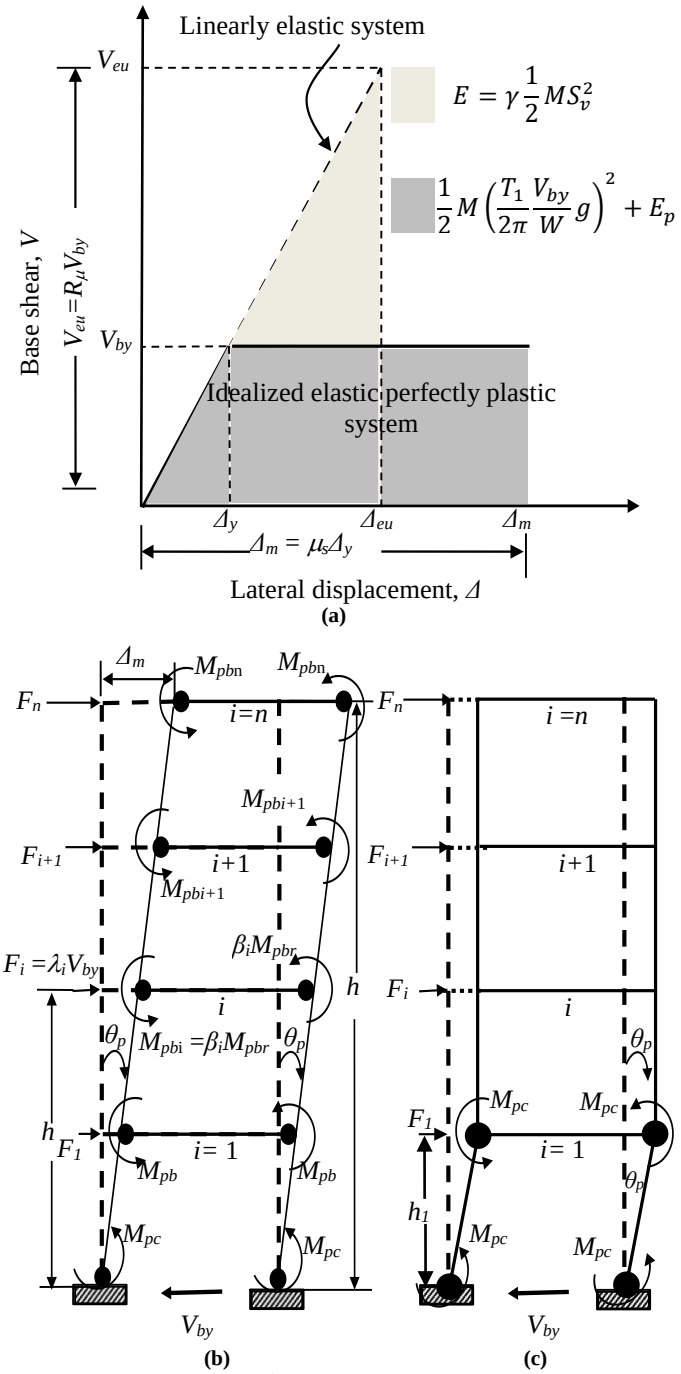

Fig. 1 (a) Concept of modified energy balance, (b) preselected yield mechanism for PBPD of SMRF, and (c) undesirable soft storey collapse mechanism.

The modified energy balance concept and preselected yield mechanism with uniform storey drift up to the target used in PBPD of steel moment resisting frames by Lee and Goel [3] is shown in Figure 1. This assumed yield mechanism follows a uniform, unidirectional inter-storey drift along the height and the energy dissipated is equal to the monotonic plastic energy demand on the system. Considering the Elastic Perfectly Plastic (EPP) response of the structural design and using the modified energy balance equation by Lee and Goel [3], the plastic energy demand (E_p) on the structural system is calculated by subtracting the elastic Strain Energy demand (E_e) from total strain Energy (E) imparted to an inelastic system as follows:

$$E_p = \frac{WT_1^2 g}{8\pi^2}\left[\gamma C_e^2 - \left(\frac{V_{by}}{W}\right)^2\right] \quad (1)$$

Where $W = M/g$ is the seismic weight of the structure, M is the total mass of the structure, T_1 is the fundamental period of the system, γ is the energy modification factor (= $[2\mu_s\text{-}1] / R_\mu^2$), μ_s is the displacement ductility ratio of the system, R_μ is the ductility reduction factor, C_e is the elastic force coefficient (= S_a/g), S_a is the design pseudo acceleration, V_{by} is the design yield base shear and g is the gravitational acceleration.

This Plastic Energy demand (E_p) is equated to the external work done by equivalent lateral forces, F_i

$$\frac{WT_1^2 g}{8\pi^2}\left[\gamma C_e^2 - \left(\frac{V_{by}}{W}\right)^2\right] = \left[\sum_{i=1}^{n} F_i h_i\right]\theta_p \quad (2)$$

Where θ_p is plastic drift and can be evaluated by deducting assumed yield drift, θ_y, from target drift, θ_t, the assumption of a suitable yield drift, θ_y, is based on the observed behaviour (under static incremental loads) of LLRS systems. Generally, steel LLRS ranges from 0.75% to 1.0% [5]. Substitution of $\lambda_i = F_i/V_{by}$ in equation (2) leads to the following quadratic equation in terms of (V_{by}/W)

$$\left(\frac{V_{by}}{W}\right)^2 + \frac{\theta_p 8\pi^2}{T_1^2 g}\left[\sum_{i=1}^{n} F_i h_i\right]\left(\frac{V_{by}}{W}\right) = \gamma C_e^2 \quad (3)$$

Where h_i is the height of i^{th} floor measured from the ground, and λ_i is the lateral force distribution factor. Since no specific recommendation for the lateral force distribution for PBPD exists, any commonly adopted distribution can be used [5]. The positive root of a quadratic equation (3) expresses the required yield base shear (V_{by}). Once V_{by} is obtained, the virtual work principle of plastic analysis is used to size the columns and beams of SMRF as follows:

$$\left[2M_{pc} + \sum_{i=1}^{n} 2M_{pbi}\right]\theta_p = V_{by}\left[\sum_{i=1}^{n} \lambda_i h_i\right] \quad (4)$$

Where M_{pc} is the plastic moment capacity of column section at bases; M_{pbi} is the plastic moment capacity of floor beams at the i^{th} level and taken as $\beta_i M_{pbr}$; where β_i is a shear proportioning factor as ratio of storey shear to base shear (= V_i / V_{by}) and M_{pbr} is plastic moment capacity of reference beam which is considered as roof beam.

The plastic moment capacity of the column section (M_{pc}) at bases can be evaluated by restricting undesirable soft-storey plastic collapse (Figure 1. c) as follows:

$$M_{pc} = \frac{V_{by} h_1}{4} \quad (5)$$

The design moment and axial force in columns at any height h are evaluated considering the moment equilibrium of free body diagrams for columns after attaining the preselected collapse mechanism.

2.2. PBPD of 21-Storey SMRF

The study building considered for PBPD is a 21-storey office building in Los Angeles, USA. The structural layout of this study building is decided after modifying the number of bays, bay widths in floor plans and the number of storeys and storey heights in elevations of 9- and 20-storey SAC buildings [25]. The floor plan of the building, shown in Figure 2, has a symmetrical square configuration with five bays in both directions. The bay width in both directions is constant and equals 8 m. The story height is 4.0 m for all floors, with a total building height of 84.0 m. SMRFs in the outer periphery are Lateral Load Resisting Systems (LLRS) for both directions ((N-E as well as S-W) excitation.

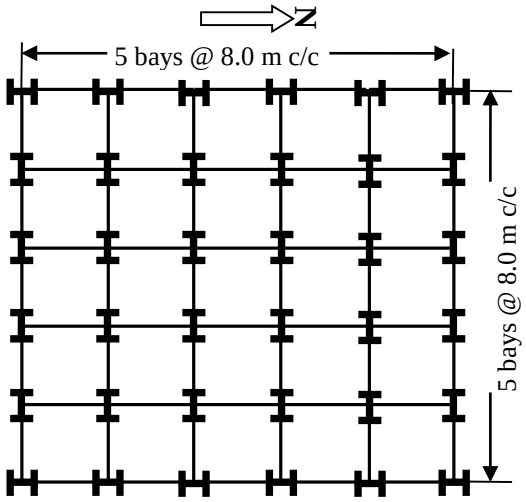

Fig. 2 Plan of the 21-storey study building with SMRF in the outer periphery as LLRS

All floors bear 9240 kN uniform seismic weight per floor. The soil at the site is considered stiff soil, with the risk category of the building as 'I'. For the seismic design of this

building, the Maximum Considered Earthquake (MCE) spectral response acceleration parameters for 0.2 sec and 1 sec are taken as SDS= 1.622g and SD1 = 0.853g, respectively, as per ASCE 7 [26].

Following the PBPD procedure of Lee and Goel [3], three design cases for this 21-storey SMRF are obtained to provide three different target displacement ductility ratios (μ_t) of 2.0, 2.5 and 3.0 with a consistent target drift of 2% using an estimated natural period of 2.37 second. These designs are respectively designated as SMRF21.2, SMRF21.2.5 and SMRF21.3. Various design parameters for these designs, as calculated using Equations 1 to 3, are shown in Table 1.

The column and beam cross sections designed as per the virtual work principle of plastic design for preselected collapse mechanism (Equations 4 and 5) are selected as broad flange sections (W-section) from the AISC steel table [27].

Table 1. Design parameters for PBPD design cases of 21-storey SMRF

Frame	(θ_t)	$\mu_t=\theta_t/\theta_y$	θ_y	θ_p	V_{by}/W
SMRF21.2.0	0.200	2.00	0.010	0.010	0.111
SMRF21.2.5	0.200	2.50	0.008	0.012	0.066
SMRF21.3.0	0.200	3.00	0.007	0.013	0.055

The structural steel specification for W-sections is ASTM A992 GR50 with yield stress, F_y = 345 MPa and ultimate stress, F_u = 450 MPa. Adequate lateral support to beam flanges is assumed from the floor diaphragm. Moreover, the cross sections for beams and columns are checked for the compact section criterion. Figure 3 summarises these PBPD designs, showing beam column sizes for each case.

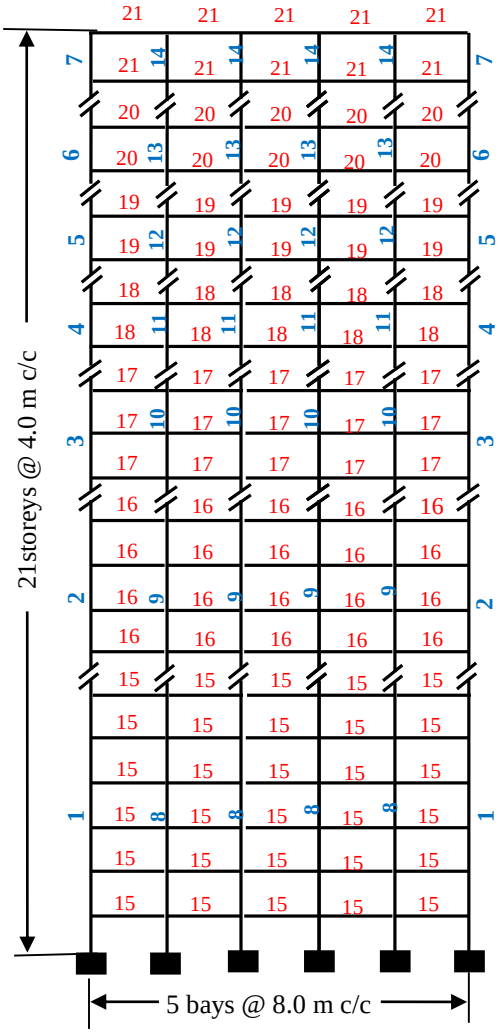

Member number	Member cross section		
	SMRF212.0	SMRF212.5	SMRF213.0
1	W 14X605	W 14X500	W 14X426
2	W 14X500	W 14X426	W 14X405
3	W 14X426	W 14X370	W 14X342
4	W 14X342	W 14X342	W 14X283
5	W 14X311	W 14X311	W 14X237
6	W 14X237	W 14X211	W 14X211
7	W 14X211	W 14X176	W 14X132
8	W 14X808	W 14X730	W 14X665
9	W 14X665	W 14X605	W 14X550
10	W 14X550	W 14X455	W 14X398
11	W 14X455	W 14X370	W 14X311
12	W 14X370	W 14X311	W 14X283
13	W 14X283	W 14X233	W 14X211
14	W 14X211	W 14X193	W 14X145
15	W 18X234	W 18X158	W 18X143
16	W 18X211	W 18X143	W 18X130
17	W 18X192	W 18X130	W 18X119
18	W 18X175	W 18X119	W 18X106
19	W 18X158	W 18X106	W 18X97
20	W 18X130	W 18X97	W 18X76
21	W 18X86	W 18X76	W 18X71

Fig. 3 Member cross sections for PBPD of SMRF21.2.0, SMRF21.2.5 and SMRF21.3.0

3. Analytical Testing of PBPD of 21-Storey SMRF and Use of Supplementary Friction Dampers

Three PBPD designs of 21-storey SMRF are analytically tested using Nonlinear Static Pushover Analysis (NSPA) and Nonlinear Time History Analysis (NTHA) to check the effectiveness of the PBPD method for high-rise LLRS. These two analyses: (i) NSPA under IBC 2018 [28] recommended seismic lateral force distribution is aimed to evaluate yield drift, θ_y and normalized base shear V_{by}/W; (ii) NTHA under suite of strong motion records is aimed to obtain plastic drift, θ_p; displacement ductility demand,(μ_d); and inter-storey drift (θ).

3.1. Analytical Modeling and Validation

Three PBPD cases of 21-storey SMRF are simulated using SAP 2000 [29]. The system is centerline modelled using a lumped mass model with 5% Rayleigh damping (in the first two modes) for the NTHA. The nominal lateral stiffness from the gravity frames is neglected. Eigenvalue analysis is carried out to evaluate the fundamental modes of vibration. Force-deformation criteria for the plastic hinges used in the NSPA and NTHA are defined based on ATC-40 [30] and FEMA356 [31] regulations. The global P-Delta effect is accounted for in the analysis. NSPA under IBC 2018 [28] recommended that seismic lateral force distribution be continued up to a worldwide drift of 4%, sufficient to cause inelastic behaviour in the SMRF system. The yield base shear, V_{by} and yield drift, $\theta_y = \Delta_y/H$ for three design cases are obtained by bi-linearization of pushover plots from NSPA. Ten near-field ground motion records consisting of the first five earthquakes from highly seismic zones of the USA and the remaining five from highly seismic areas of the globe are used to perform NTHA of these design cases. The moment magnitude of these earthquakes lies between 5.5 Mw and 7.9 Mw, representing moderate to high seismicity. For the NTHA of each design case, these acceleration time histories are scaled through Scale Factor (SF) to have the same design spectral acceleration at the assumed fundamental period. Thus, the Scale Factor (SF) for each Ground Motion (GM) is calculated as:

$$SF = \frac{S_a(T_1)_{Design}}{S_a(T_1)_{GM}} \tag{6}$$

$S_a(T_1)_{Design}$ is designed spectral acceleration corresponding to the assumed fundamental period T_1, and $S_a(T_1)_{GM}$ is ground motion spectral acceleration related to the same fundamental time period T_1. Details of these ground motion records and scale factors are provided in Table 2.

Table 2. Details of strong motion record for NTHA of 21-storey SMRF

Earthquake	Country	Station	Date	Magnitude (Mw)	PGA (*g*)	SF
San Fernando	USA	Pacoima Dam	Feb. 9, 1971	6.6	1.450	2.47
Imperial Valley	USA	El Centro Array #8	Oct. 15, 1979	6.5	0.538	3.43
Whittier Narrows	USA	Santa Fe Springs	Oct. 01, 1987	5.9	0.433	3.53
Lander	USA	Lucerne	June 28, 1992	7.3	0.721	2.63
Northridge	USA	Newhall	Jan. 17, 1994	6.7	0.698	3.37
Kobe	Japan	Takarazuka	Jan. 16, 1995	6.9	0.707	3.18
Chi Chi	Taiwan	TCU065	Sept. 20, 1999	7.7	0.831	2.95
Kocaeli	Turkey	Sakarya	Aug. 17,1999	7.6	0.376	4.19
Düzce	Turkey	Düzce	Nov. 12,1999	7.2	0.427	4.34
Tabas	Iran	Tabas	Sept. 16, 1978	7.4	0.851	2.68

(Source: https://peer.berkeley.edu/peer-strong-ground-motion-databases and https://www.strongmotioncenter.org)

Using NTHA, the mean value of plastic drift, θ_p and displacement ductility demand, μ_d, are calculated as:

$$\theta_p = \frac{\Delta_m - \Delta_y}{H} \tag{7}$$

$$\mu_d = 1 + \frac{\theta_p}{\theta_y} \tag{8}$$

Where Δ_y = yield roof displacement obtained from NSPA, H = total height of SMRF and Δ_m = mean value of maximum roof displacement at an instant of maximum inter-storey drift obtained from NTHA under selected ten vital motion records. Table 3 summarises the fundamental time period, T obtained from eigenvalue analysis and yield drift, θ_y, and normalized base shear Vby/W obtained from NSPA for three PBPD cases of 21-storey SMRF. It also includes the mean value of plastic drift, θ_p and displacement ductility

demand, $\mu_{d,}$ obtained through NTHA under ten vital motion records selected. It can be observed that the fundamental time period, $T_{1,}$ obtained from eigenvalue analysis, yield drift, θy, and normalized base shear V_{by}/W from NSPA are nearly close to the assumed/calculated value in the design procedure. Moreover, the mean value of displacement ductility demand, $\mu_{d,}$ is in close agreement with the target values, as mentioned in the design parameters of Table 1.

Table 3. Results obtained from eigenvalue, NSP and NTH analysis of 21-storey SMRF

Frame	Eigen Value Analysis	NSPA		NTHA	
	T_1 (s)	θ_y	V_{by}/W	Mean value of θ_p	Mean value of μ_d
SMRF21.2.0	2.43	0.007	0.092	0.006	1.86
SMRF21.2.5	2.47	0.008	0.067	0.010	2.25
SMRF21.3.0	2.58	0.010	0.054	0.017	2.70

Maximum inter-storey drifts for each design case as obtained through NTHA under the suite of ten strong motions are statistically processed to obtain the Mean - Standard Deviation (M-SD); Mean (M) and represent + Standard Deviation (M+SD) values of maximum inter-storey drift. Considering normal probability distribution, the maximum inter-storey drift values between (M±SD) indicate about 66% of importance in this range. This can be considered an adequate basis for evaluating maximum inter-storey drifts under moderate to vital ground motion records. These drifts are plotted against respective target drifts in Figure 4. For the bottommost storeys in all three PBPD design cases, the Mean (M) and Mean + Standard Deviation (M+SD) inter-storey drifts obtained through NTHA exceeded the preselected target value.

PBPD design cases with higher displacement ductility demand like SMRF21.2.5 and SMRF21.3.0, the inter-storey drift distribution is non-uniform with a large concentration of inelastic drift at the bottom, which is attributed to dominance of P-Delta and higher modes effect. The analytical testing of PBPD frames of 21-storey reflects that the preselected performance objective in target uniform drift is partially achieved, which enforces the use of supplementary damping devices for economical PBPD frames offering uniform inter-storey drift distribution within the target drift.

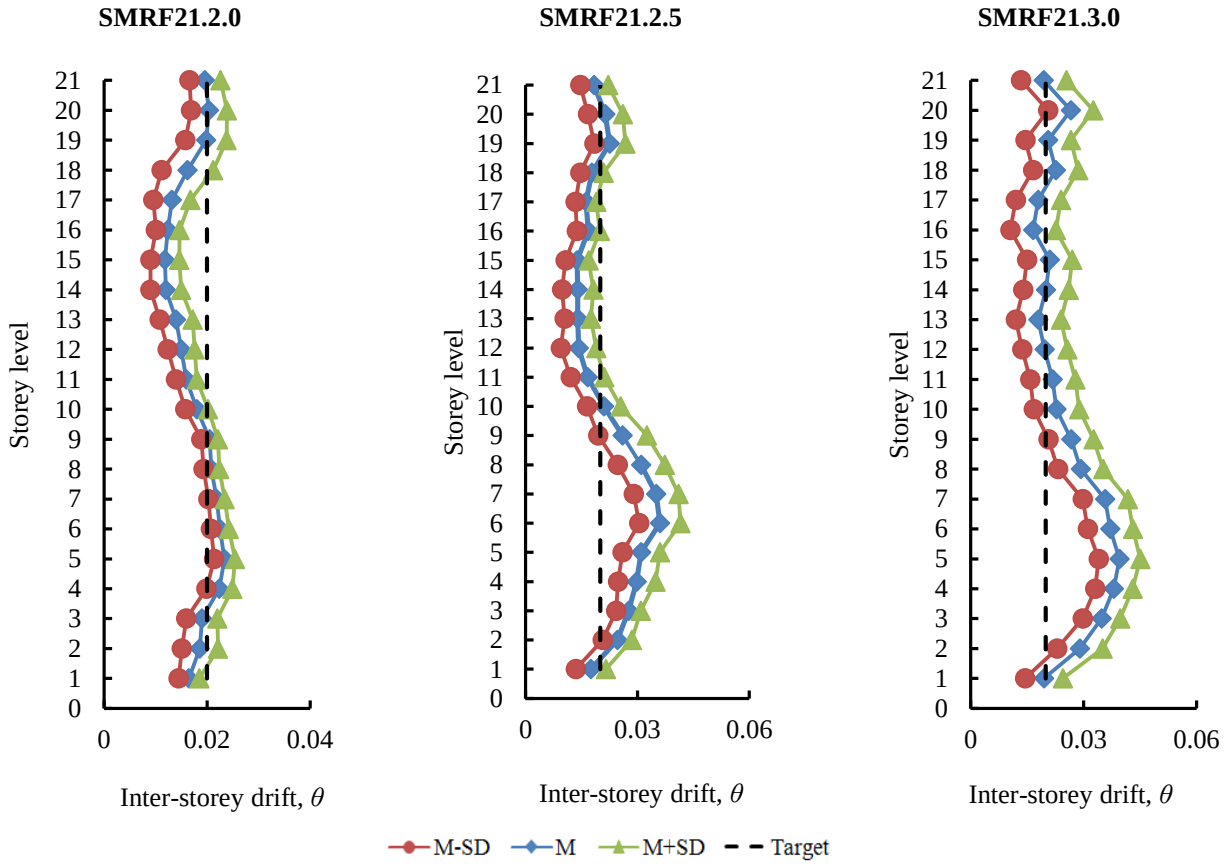

Fig. 4 M±SD values of maximum inter-storey drift for three PBPD cases of 21-storey SMRF under the suite of ten strong motions

3.2. Use of Supplementary Friction Dampers

The exclusion of P-Delta and higher mode effect in formulating the PBPD approach hampers the method's effectiveness for high-rise SMRF where it fails to achieve the preselected performance objectives regarding uniform inter-storey drift within the target. Hence, a supplementary friction damper is proposed to control the excessive inelastic drift and ensure its smooth and consistent distribution across the structure's height for a 21-storey SMRF designed per the PBPD approach. Pall friction dampers [9] consisting of diagonal friction devices with single tension/compression braces are selected as supplementary friction devices in this study. Figure 5 shows the schematic of a friction damper in single diagonal tension/compression bracing, its hysteresis characteristics and real-life application in Moscone West Convention Center, San Francisco, USA [28].

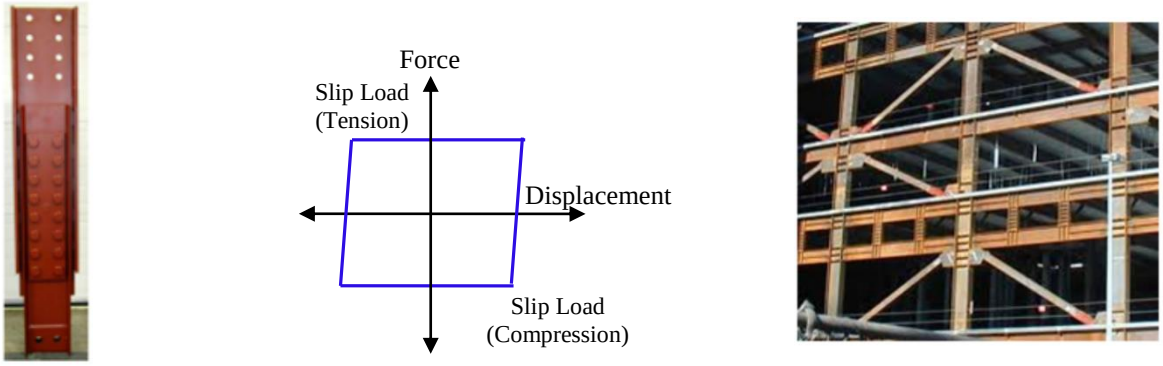

(a) **(b)** **(c)**

Fig. 5 Pall friction dampers: (a) schematic in the form of single diagonal tension/compression bracing, (b) hysteresis characteristics, and (c) real-life application in Moscone West Convention Center, San Francisco, USA [34].

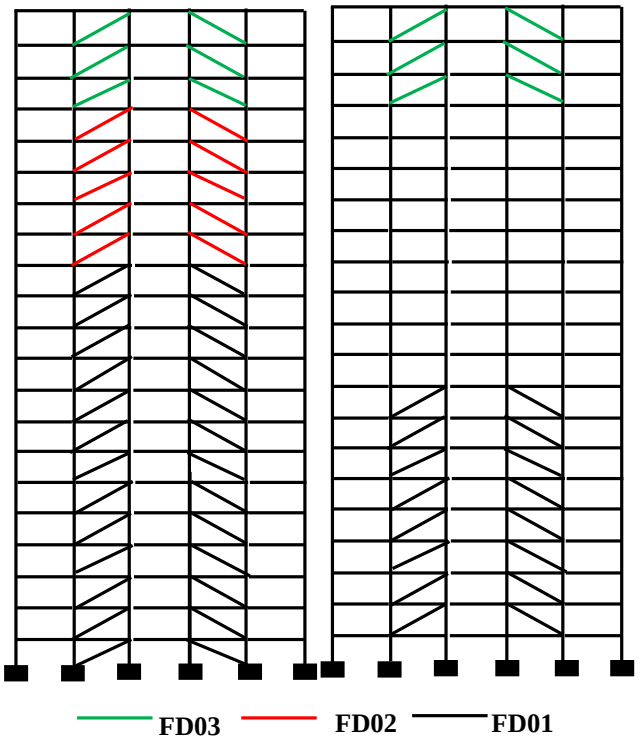

(a) (b)

Fig. 6 Two distinct configurations of friction dampers in 21-storey SMRF (a) fully-equipped friction dampers, and (b) partially-equipped friction dampers (friction dampers in 2nd to 9th storeys and topmost 3 storeys).

As per Baktash and Marsh [33], for a diagonal friction damper as a single tension/compression brace, the shear force exerted by braces is 50% of the total shear force exerted by the frame and braces. The slip load is estimated at 1/3 of the story shear, ensuring that the ratio of lateral brace stiffness to total lateral story stiffness (frame + braces) is strictly greater than 0.5. Wen link model with yielding exponent, *exp* = 10 and post-yield stiffness ratio of, *r* = 0.0001, as suggested by Pall [32-33], is used to analytically simulate the friction damper in SAP 2000 [31]. These suggested values of yielding exponent and post-yield stiffness result in a rectangular hysteresis loop of friction damper, as represented in Figure 5(b). Friction-damped braces are designed to have yield strength equal to the slip load of the friction dampers. Table 4 provides the properties of friction dampers used in this study.

Table 4. Properties of friction dampers used for PBPD cases of 21-storey SMRF

Frame	Friction damper	Slip force (kN)	Stiffness (kN/m)	Mass (kg)
S21.2.0	FD01	5600	260000	5400
	FD02	4900	170000	4700
	FD03	3100	80000	3100
S21.2.5	FD01	4000	190000	3900
	FD02	3500	130000	3400
	FD03	2300	50000	2300
S21.3.0	FD01	3200	160000	3100
	FD02	2700	100000	2600
	FD03	1800	40000	1700

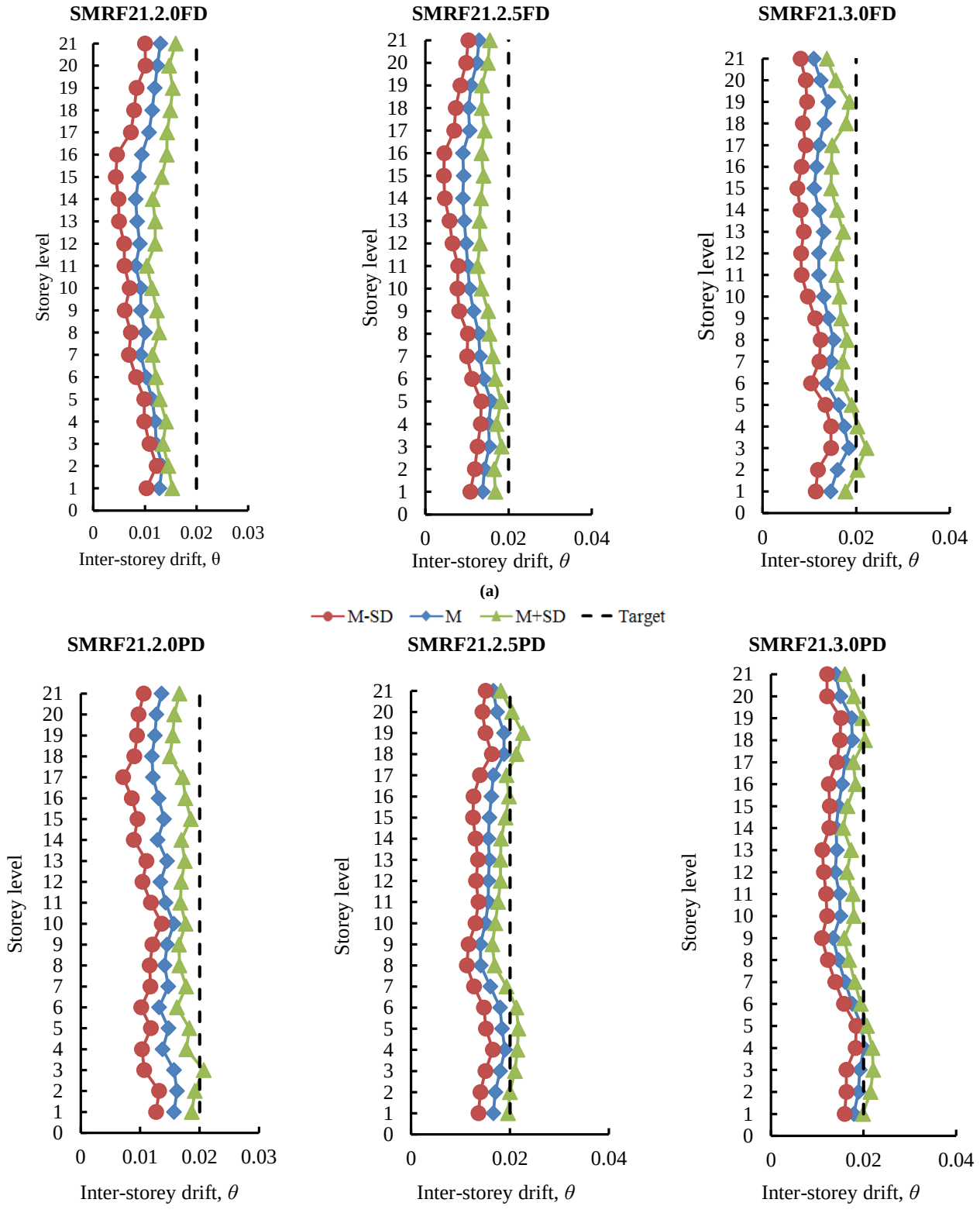

Fig. 7 M±SD values of maximum inter-storey drift for three PBPD cases of 21-storey SMRF under the suite of ten strong motions: a) with fully-equipped friction dampers, and (b) with partially-equipped friction dampers.

For 21-storey SMRF, these friction dampers are provided in two distinct configurations as follows: (i) initially, friction dampers in two bays (each for tension and compression) are installed in all storeys of three PBPD frames irrespective of maximum inter-storey drifts obtained from NTHA (Figure 4). Friction dampers: FD01 from ground to 12th storey level; FD02 from 13th to 18th storey level; and FD03 from 19th storey to 21st storey level are used for this configuration.

These frames are considered to be fully equipped with friction dampers and respectively designated as SMRF21.2.0FD, SMRF21.2.5FD and SMRF21.3.0FD; (ii) in later design, friction dampers are provided in partial storeys considering the primarily concentrated residual inter-storey drifts. It can be observed from Figure 4 for the 2nd to 9th storeys and the topmost three storeys where maximum inter-storey implications are exceeded or very close to the assumed uniform target drift. Friction dampers: FD01 from the 1st to the 9th storey level and FD03 from the 18th to the 21st are used for this configuration. Partly equipped with friction dampers, these frames are SMRF21.2.0PD, SMRF21.2.5PD and SMRF21.3.0PD.

Figure 6 represents a schematic of these configurations. NTHA analyzes these fully and partially equipped friction damper PBPD frames of the 21-storey building under identical ground motion records (Table 2). This analysis is intended to check the effectiveness of supplementary damping devices to control the excessive inelastic drift and to ensure preselected uniform drift distribution in the PBPD of high-rise SMRF.

The maximum inter-storey drift distributions at an instant of maximum roof displacement, as obtained through NTHA for each design case of these two distinct configurations, are represented in Figure 7. For PBPD frames with friction dampers in all storeys (SMRF21.2.0FD, SMRF21.2.5FD and SMRF21.3.0FD), the inter-storey drift distributions are found to be near to uniform and much within the target values.

Such performance is attributed to the fact that energy dissipation by supplementary friction dampers in all 21 storeys dominates the energy dissipation due to the yielding of the frame, which led to a conservative design as the significant inelastic deformation capacity of the system is suppressed.

In the case of PBPD frames with partially-equipped friction dampers (SMRF21.2.0PD, SMRF21.2.5PD and SMRF21.3.0PD), these inter-storey drift distributions are almost uniform and tend to target which prove to be more economical due to simultaneous energy dissipation by both yielding of frame and by supplementary friction.

4. Seismic Collapse Vulnerability Assessment

The maximum inter-storey drift (θ_{max}) limits for the life safety (LS) performance = 2.5%, and the collapse prevention (CP) performance = 5% as per ASCE 41 [34] is used to assess the seismic collapse susceptibility of PBPD designs of 21-storey SMRF with and without supplemental friction damper. Nonlinear Multi-record Incremental Dynamic Analysis (MIDA) followed by seismic fragility analysis corresponding to Collapse Prevention (CP) limit state is used for this purpose.

4.1. Multi-record Incremental Dynamic Analysis (MIDA)

To offer an appropriate level of record-to-record randomization for the seismic performance assessment of structures on firm soil and sensitive to near-source solid earthquakes, a set of 20 "Large Magnitude Small Distance" (LMSR) records is selected for MIDA. These LMSR ground motion records characterized by magnitudes in the range of 6.5 - 6.9 Mw and epicentral distances in the field of 16-32 km were used in several past investigations [35–37].

Table 5 provides details of LMSR vital motion records. For each earthquake record of the LMSR series, the Incremental Dynamic Analysis (IDA) is carried out by scaling up ground acceleration time history till global collapse. The scaling of each record is aimed to cover the entire range of structural response, from elasticity to yielding, and finally, global dynamic instability.

For MIDA plots, the elastic force coefficient (C_e=S_a/g) corresponding to the fundamental mode period, T_1 and damping ξ = 5 % is considered as the Intensity Measure (IM) and maximum inter-story drift (θ_{max}) is selected as the Damage Measure (DM).

Figure 8 provides the LMSR-based MIDA curve of all nine PBPD frames of 21-storey SMRF with and without supplemental friction damper. Each IDA curve demonstrates how each PBPD frame performs seismically under seismic demand imposed upon the structure by each ground motion record at various intensities.

The mean IDA curve for each PBPD frame is highlighted with a thick black line in MIDA plots; three different drift limits, namely: Target (θ_{max} = θ_t); LS (θ_{max} = 2 %) and CP (θ_{max} = 5 %), are shown to asses collapse susceptibility of the frame.

The intersection of the mean IDA curve with these drift limits, as highlighted with an orange circle, provides a range Intensity Measure (IM) in terms of first-mode spectral acceleration (S_a/g). The flat line in IDA plots indicates excessive drift occurs under small increases in ground motion intensity, signalling the onset of dynamic instability, which can be considered a complete frame collapse.

Table 5. Details of LMSR vital motion records

No	Identifier	Event	Year	Station	f^1 (°)	M^2	R^3 (km)	PGA (g)
1	LP1	Loma Prieta	1989	Agnews State Hospital	90	6.9	28.2	0.159
2	IV1	Imperial Valley	1979	Plaster City	135	6.5	31.7	0.057
3	LP2	Loma Prieta	1989	Hollister Diff. Array	255	6.9	25.8	0.279
4	LP3	Loma Prieta	1989	Anderson Dam	270	6.9	21.4	0.244
5	LP4	Loma Prieta	1989	Coyote Lake Dam	285	6.5	22.3	0.179
6	IV2	Imperial Valley	1979	Cucapah	85	6.9	23.6	0.309
7	LP5	Loma Prieta	1989	Sunnyvale Colton Ave	270	6.9	28.8	0.207
8	IV3	Imperial Valley	1979	El Centro Array #13	140	6.5	21.9	0.117
9	IV4	Imperial Valley	1979	Westmoreland Fire Station	90	6.5	15.1	0.074
10	LP6	Loma Prieta	1989	Hollister South & Pine	0	6.9	28.8	0.371
11	LP7	Loma Prieta	1989	Sunnyvale Colton Ave	360	6.9	28.8	0.209
12	SH1	Superstition Hills	1987	Wildlife Liquefaction Array	90	6.7	24.4	0.180
13	IV5	Imperial Valley	1979	Chihuahua	282	6.5	28.7	0.254
14	IV6	Imperial Valley	1979	El Centro Array #13	230	6.5	21.9	0.139
15	IV7	Imperial Valley	1979	Westmoreland Fire Station	180	6.5	15.1	0.110
16	LP8	Loma Prieta	1989	WAHO	0	6.9	16.9	0.370
17	SH2	Superstition Hills	1987	Wildlife Liquefaction Array	360	6.7	24.4	0.200
18	IV8	Imperial Valley	1979	Plaster City	45	6.5	31.7	0.042
19	LP9	Loma Prieta	1989	Hollister Diff. Array	165	6.9	25.8	0.269
20	LP10	Loma Prieta	1989	WAHO	90	6.9	16.9	0.638

[1] Component, [2] Moment Magnitudes, [3] Closest Distances to Fault Rupture

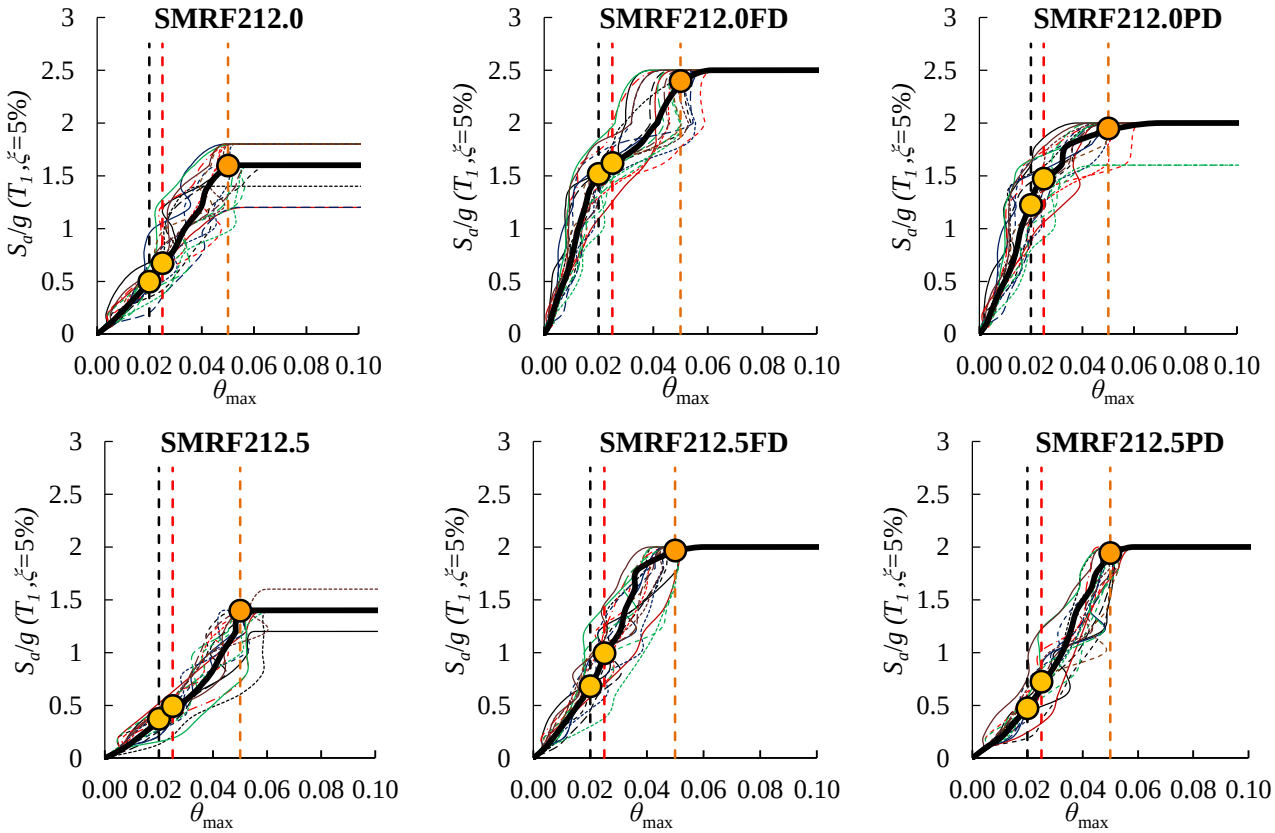

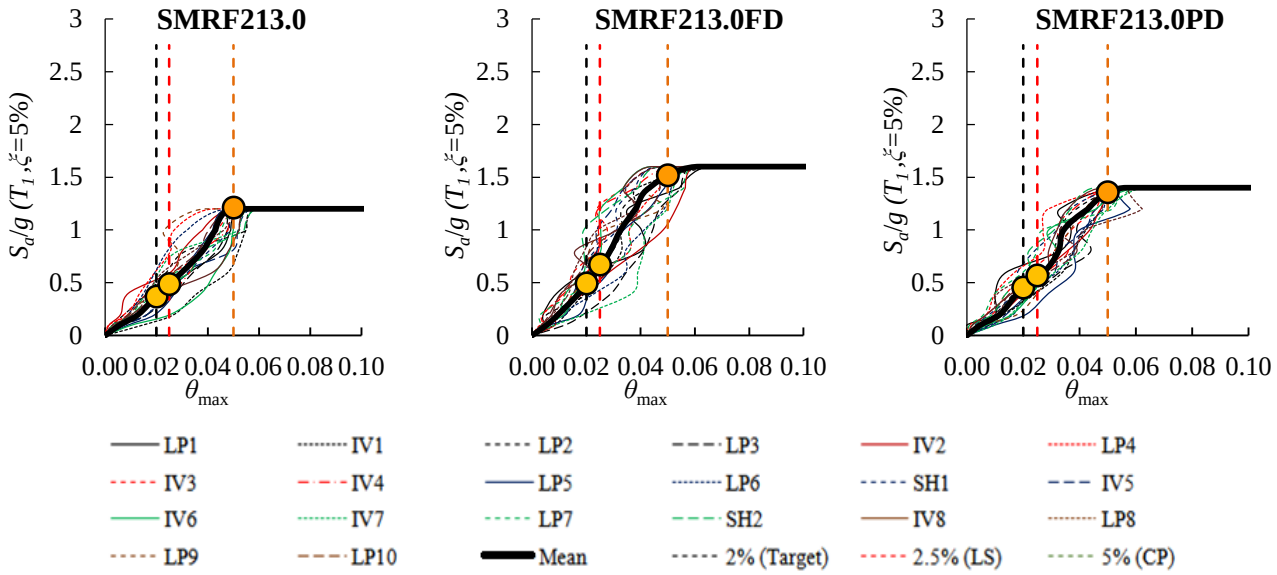

Fig. 8 LMSR-based MIDA curves for PBPD frames with and without supplementary friction dampers

As observed from MIDA plots, the PBPD designs without friction dampers (SMRF212.0; SMRF212.5 and SMRF213.0) have attained global dynamic instability even before θ_{max} = 5 %, the maximum inter-storey drift limit corresponding to Collapse Prevention (CP) performance.

The complete collapse in these frames is observed in the Intensity Measure (IM) range of S_a (T_1, ξ = 5%) = 1.20g –1.50g. Frames having friction dampers in all storeys (SMRF21.2.0FD, SMRF21.2.5FD and SMRF21.3.0FD) as well those equipped with dampers in selected partial storeys (SMRF21.2.0PD, SMRF21.2.5PD and SMRF21.3.0PD) are successful in attaining the maximum inter-storey drift limit of collapse prevention without any dynamic instability. The seismic performance of PBPD frames with supplementary friction dampers is compared to that of bare PBPD frames (without friction dampers) in Table 6.

For PBPD frames with dampers, characteristic flattening of the mean IDA curve representing complete collapse is observed to be in the relatively higher range of IM (1.45g –2.45g for fully equipped configuration and 1.30g –1.80g for partially equipped configuration) when compared with frames without supplementary friction dampers.

Table 6. Seismic performance of PBPD frames with and without supplementary friction dampers

Frames	Storeys with damper	IM = S_a (T_1, ξ = 5 %)			Performance prior to CP
		$(\theta_{max})_{Target}$ = 2%	$(\theta_{max})_{LS}$ = 2.5%	$(\theta_{max})_{CP}$ = 2.5%	
SMRF212.0	None	0.49g	0.62g	1.50g	Collapse
SMRF212.0FD	All	1.47g	1. 57g	2.45g	Gradual yielding and hardening
SMRF212.0PD	1st to 9 and 18th to 21st	1.23g	1.49g	1.80g	Gradual yielding and softening
SMRF212.5	None	0.39g	0.47g	1.23g	Collapse
SMRF212.5FD	All	0.76g	0.94g	2.00g	Gradual yielding and hardening
SMRF212.5PD	1st to 9 and 18th to 21st	0.50g	0.72g	1.78g	Gradual yielding and softening
SMRF213.0	None	0.36g	0.44g	1.20g	Collapse
SMRF213.0FD	All	0.51g	0.73g	1.45g	Gradual yielding and hardening
SMRF213.0PD	1st to 9 and 18th to 21st	0.42g	0.46g	1.30g	Gradual yielding and softening

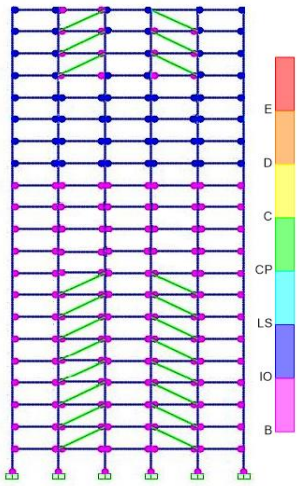

Fig. 9 Typical yielding mechanism for SMRF213.0PD under LP20 at IM = S_a (T_1, ξ = 5 %) = 1.30g

Figure 9 provides the typical yielding mechanism for SMRF213.0PD under LP20 record (Earthquake: 1989 Loma Prieta, Station WAHO) at IM = S_a (T_1, ξ = 5 %) = 1.30g. For this higher displacement ductility demand, the PBPD frame installed with supplementary friction dampers in partial storeys (FD01 from 1st to 9th storey and FD03 from 18th storey to 21st storey), the plastic hinges rotation at the ends of floor beam and the bases of columns are well within limits of LS as well as the preselected performance objectives of PBPD approach are effectively achieved. Thus, inter-storey drift demands and yielding mechanisms observed from MIDA justify the effectiveness of supplementary friction dampers in selected storeys of PBPD frames to control the likelihood of collapse and attainment of pre-decided performance objectives.

4.2. Seismic Fragility Analysis

To evaluate the likelihood of collapse in terms of IM = S_a (T_1, ξ = 5 %), the fragility curve was derived from the findings of MIDA as per Porter et al. [38] and Baker [39]. According to Baker [39], the cumulative probability of collapse corresponding to IM can be expressed as

$$P_{[\text{collapse/IM} = x]} = \Phi\left[\frac{\ln(x/\theta)}{\beta}\right] \quad (9)$$

Where $P_{[\text{collapse/IM = x}]}$ is the probability (likelihood) of collapse; $\Phi[\,]$ is the normal cumulative distribution function; θ is the median of the fragility function (the IM level with 50% probability of collapse); and β is the standard deviation of ln (IM) referred to as the dispersion of IM. The results of MIDA are used to estimate the fragility function parameters (θ and β) by taking logarithms of each ground motion's IM value associated with the onset of collapse as follows:

$$\ln\theta = \frac{1}{n}\sum_{i=1}^{n} \ln \text{IM}_i \quad (10)$$

$$\beta = \sqrt{\frac{1}{n-1}\sum_{i=1}^{n}\left(\ln\left(\text{IM}_i/\theta\right)\right)^2} \quad (11)$$

Where n is the number of ground motions considered, and IM_i is the intensity measure value associated with one collapse set for i^{th} ground motion.

Figure 10 compares the seismic fragility of all 21-story bare PBPD frames (corresponding to collapse at θ_{max} = 5%) with the fragility of structures equipped with supplementary friction dampers in all and partial storeys. As observed, the bare PBPD frames (SMRF2 12.0; SMRF212.5 and SMRF213.0) have a much higher probability of collapse than those outfitted with additional friction dampers for given seismic demands.

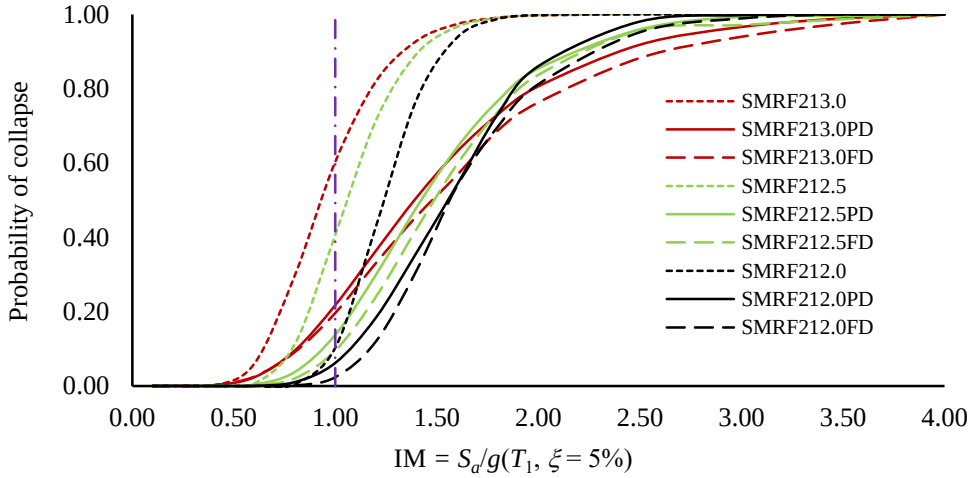

Fig. 10 Fragility curves for PBPD frames with and without supplementary friction dampers

Table 7. Probabilities of collapse PBPD frames with and without supplementary friction dampers for IM = S_a (T_1, ξ = 5 %) = 1.00g

Design	Probability of collapse		
	Bare: Without Dampers	Fully: Dampers in All Storeys	Partially: Dampers in Selected Storeys
SMRF212.0	12.27%	2.38%	6.21%
SMRF212.5	40.68%	9.51%	13.78%
SMRF213.0	60.34%	19.65%	21.78%

Probabilities of collapse for all nine PBPD frames corresponding to IM = S_a (T_1, ξ = 5 %) = 1.00g, are summarized in Table 7. Using supplementary friction dampers in all storeys reduces the probability of collapse of bare PBPD frames by almost 65% to 80 %, with a higher reduction for SMRF212.0.

For PBPD designs with higher displacement ductility ratios (SMRF213.0 and SMRF212.5), there is no significant difference in the probability of collapse for frames equipped with dampers in all and in selected storeys. Hence, using supplementary friction damper in selected storeys of large concentrated residual drifts from NTHA is a more efficient strategy to minimize the probability of collapse of PBPD frames.

5. Concluding Summary

Due to the predominance of higher mode and P-Delta effects, PBPD designs of medium to high-rise SMRF for higher ductility demands are prone to develop substantially concentrated and non-uniform inter-storey drifts. The use of supplementary friction dampers to control the primarily focused non-uniform inter-storey drift of highly flexible SMRF designed as per the PBPD approach is proposed in this analytical research. Three PBPD design cases of a 21-storey SMRF for target displacement ductility ratios μ_t = 2.0, 2.5 and 3.0 are analytically tested using NSPA and NTHA for ascertaining the use of supplementary friction dampers.

Two distinct configurations for using supplemental friction dampers in bare SMRFs designed by the PBPD approach are adopted. For fully-equipped structures, friction dampers are installed in all storeys, and in partially-equipped configurations, dampers are used in selected storeys of significant concentrated residual drift induced through NTHA.

The LMSR-based MIDA is carried out to compare the seismic performance of bare frames with frames equipped with supplementary friction dampers. The likelihood of seismic collapse of bare as friction damper provided structure is assessed through the fragility analysis using the results of MIDA. The following outcomes are summarized based on present analytical research.

- From NTHA of 21-storey bare PBPD frames with greater displacement ductility demands, such as SMRF21.2.5 and SMRF21.3.0, it is observed that the inter-storey drift distribution is non-uniform with a substantial concentration of inelastic drift in the bottommost storey. This is attributed to P-Delta dominance and higher modes effect for high-rise flexible SMRF. Hence, supplementary friction dampers to control the excessive inelastic drift and to increase the seismic energy dissipation capacity are often needed for the flexible SMRF designed with the PBPD approach.
- For PBPD frames with friction dampers in all storeys, SMRF21.2.0FD, SMRF21.2.5FD and SMRF21.3.0FD, the inter-storey drift distributions are found to be almost uniform and much within the target values. However, this Fully-equipped Dampers (FD) configuration in all storeys led to a conservative design as the significant inelastic deformation capacity of SMRF is suppressed by energy dissipation offered by supplementary friction dampers. The PD configuration where supplemental friction dampers are installed in selected drift-prone storeys of 21-storey SMRF (SMRF21.2.0PD, SMRF21.2.5PD and SMRF21.3.0PD) proves to be more economical and efficient to achieve preselected performance objectives in terms of uniform target drift and yield mechanism.
- The seismic performance of bare and friction damper installed PBPD frame evaluated through LMSR-based MIDA reflects that plain PBPD frames attain global dynamic instability even before θ_{max} = 5 %, the maximum inter-storey drift limit corresponding to Collapse Prevention (CP) performance. PBPD frames with Friction Dampers in all storeys (FD configuration) as well as in selected storeys (PD configuration) are much more effective in attaining Collapse Prevention (CP) performance without any dynamic instability.
- The seismic fragility analysis underlines the effectiveness of supplementary friction dampers in PBPD frames, as the probability of collapse is much lesser than in bare PBPD frames. Moreover, using an additional friction damper in selected drift-prone storeys was an efficient strategy to minimize the seismic damages as the vulnerability of collapse for both FD and PD configurations is insignificant.

The present research findings are limited to using supplementary Pall friction dampers for the PBPD design of a 21-storey SMRF. The effectiveness of various types of seismic dampers (such as dense, visco-elastic, lead, magnetic, and shape memory alloy) need to be assessed for different ranges of medium to high-rise SMRF designed by the PBPD approach.

Acknowledgments

The authors thank friends and colleagues from the GCOEAR, Awasari; SGU, Kolhapur; and KLE Technological University, Hubballi, for supporting the research above.

Author's Contribution

Conceptualization: S. B. Kharmale, C. S. Patil, and V. B. Patil; Analytical investigation: S. B. Kharmale and C. S. Patil; Data processing and interpretation: S. B. Kharmale and C. S. Patil; Drafting the article: S. B. Kharmale; Review and editing: S. B. Kharmale, C. S. Patil, and V. B. Patil. All authors have read and agreed to the published version of the manuscript.

References

[1] Robert Tremblay et al., "Performance of Steel Structures during the 1994 Northridge Earthquake," *Canadian Journal of Civil Engineering*, vol. 22, no. 2, pp. 338-360, 1995. [CrossRef] [Google Scholar] [Publisher Link]

[2] E. Watanabe et al., "Performances and Damages to Steel Structures during 1995 Hyogoken-Nanbu Earthquake," *Engineering Structures*, vol. 20, no. 4-6, pp. 282-290, 1998. [CrossRef] [Google Scholar] [Publisher Link]

[3] Seon Sik Lee, and Subhash C. Goel, *Research Report No. UMCEE 01-17: Performance-Based Design of Steel Moment Frames using Target Drift and Yield Mechanism*, Department of Civil and Environmental Engineering University of Michigan, Ann Arbor, MI, USA, 2001. [Google Scholar]

[4] Shih-Ho Chao, and Subhash C. Goel, *Research Report No. UMCEE 05-05: Performance-Based Design of EBF using Target Drift and Yield Mechanism*, Department of Civil and Environmental Engineering University of Michigan, Ann Arbor, MI, USA, 2005. [Google Scholar] [Publisher Link]

[5] Subhash C. Goel, and Shih-Ho Chao, "*Performance-Based Plastic Design: Earthquake-Resistant Steel Structures,*" 1st ed., International Code Council, Washington, USA, 2008. [Google Scholar] [Publisher Link]

[6] Shih-Ho Chao, Netra B. Karki, and Dipti R. Sahoo, "Seismic Behavior of Steel Buildings with Hybrid Braced Frames," *Journal of Structural Engineering*, vol. 139, no. 6, pp. 1019-1032, 2012. [CrossRef] [Google Scholar] [Publisher Link]

[7] Douglas K. Nims, Phillip J. Richter, and Robert E. Bachman, "The Use of the Energy Dissipation Restraint for Seismic Hazard Mitigation," *Earthquake Spectra*, vol. 9, no. 3, pp. 467-489, 1993. [CrossRef] [Google Scholar] [Publisher Link]

[8] G. W. Housner et al., "Structural Control: Past, Present, and Future," *Journal of Engineering Mechanics*, vol. 122, no. 9, pp. 897-971, 1997. [CrossRef] [Google Scholar] [Publisher Link]

[9] Avtar S. Pall, and Cedric Marsh, "Response of Friction Damped Braced Frames," *Journal of Structural Division*, vol. 108, no. 6, pp. 1313-1323, 1982. [CrossRef] [Google Scholar] [Publisher Link]

[10] A. Filiatrault, and S. Cherry, "Performance Evaluation of Friction Damped Braced Steel Frames under Simulated Earthquake Loads,'' *Earthquake Spectra*, vol. 3, no. 1, pp. 57-87, 1987. [CrossRef] [Google Scholar] [Publisher Link]

[11] A. Filiatrault, and S. Cherry, "Seismic Design Spectra for Friction Damped Structures," *Journal of Structural Division*, vol. 116, no. 5, pp. 1334-1355, 1990. [CrossRef] [Google Scholar] [Publisher Link]

[12] Piero Colajanni, and Maurizio Papia, "Seismic Response of Braced Frames with and without Friction Dampers," *Engineering Structures*, vol. 17, no. 2, pp. 129-140, 1995. [CrossRef] [Google Scholar] [Publisher Link]

[13] Esra Mete Güneyisi, Mario D'Aniello, and Raffaele Landolfo, "Seismic Upgrading of Steel Moment-Resisting Frames by Means of Friction Devices," *The Open Construction and Building Technology Journal*, vol. 8, no. 6, pp. 289-299, 2014. [CrossRef] [Google Scholar] [Publisher Link]

[14] Andrei M. Reinhorn, C. Li, and M. C. Constantinou, "*Experimental and Analytical Investigation of Seismic Retrofit of Structures with Supplemental Damping: Part II-Friction devices*," Buffalo (NY), State University of New York at Buffalo, 1995. [Google Scholar] [Publisher Link]

[15] Imad H. Mualla, and Borislav Belev, "Performance of Steel Frames with A New Friction Damper Device under Earthquake Excitation," *Engineering Structures*, vol. 24, no. 3, pp. 365–371, 2002. [CrossRef] [Google Scholar] [Publisher Link]

[16] Habib Saeed Monir, and Keyvan Zeynali, "A Modified Friction Damper for Diagonal Bracing of Structures," *Constructional Steel Research*, vol. 87, pp. 17-30, 2013. [CrossRef] [Google Scholar] [Publisher Link]

[17] Rosario Montuori, Elide Nastri, and Vincenzo Piluso, "Theory of Plastic Mechanism Control for the Seismic Design of Braced Frames Equipped with Friction Dampers," *Mechanics Research Communications*, vol. 58, pp. 112-123, 2014. [CrossRef] [Google Scholar] [Publisher Link]

[18] M. Latour, V. Piluso, and G. Rizzano, "Experimental Analysis on Friction Materials for Supplemental Damping Devices," *Construction and Building Materials*, vol. 65, pp. 159-176, 2014. [CrossRef] [Google Scholar] [Publisher Link]

[19] Lucia Tirca, "Friction Dampers for Seismic Protections of Steel Buildings Subjected to Earthquakes: Emphasis on Structural Design," *Encyclopedia of Earthquake Engineering*, Springer, Berlin, Heidelberg, pp. 1058–1070, 2015. [CrossRef] [Google Scholar] [Publisher Link]

[20] Majd Armaly et al., "Effectiveness of Friction Dampers on the Seismic Behavior of High Rise Building vs Shear Wall System," *Engineering Reports*, vol. 1, no. 5, pp. 1-14, 2019. [CrossRef] [Google Scholar] [Publisher Link]

[21] Avtar Pall, "*The Making of Mega Pall Friction Dampers for Torre Cuarzo Office Tower in Mexico City*," 16th World Conference on Earthquake Engineering, Santiago, Chile, 2017. [Google Scholar] [Publisher Link]

[22] Sutat Leelataviwat, Subhash C. Goel, and Božidar Stojadinović, "Toward Performance-Based Seismic Design of Structures," *Earthquake Spectra*, vol. 15, no. 3, pp. 435-461, 1999. [CrossRef] [Google Scholar] [Publisher Link]

[23] W.C. Liao, and S.C. Goel, "Performance-Based Seismic Design of RC SMF Using Target Drift and Yield Mechanism as Performance Criteria," *Advances in Structural Engineering*, vol. 17, no.4, pp. 85-97, 2014. [CrossRef] [Google Scholar] [Publisher Link]

[24] Watchara Chan-Anan, Sutat Leelataviwat, and Subhash C. Goel, "Performance-Based Plastic Design Method for Tall Hybrid Coupled Walls," *The Structural Design of Tall and Special Buildings*, vol. 25, no. 14, pp. 681-699, 2016. [CrossRef] [Google Scholar] [Publisher Link]

[25] Akshay Gupta, *Seismic Demands For Performance Evaluation of Steel Moment Resisting Frame Structures*, Department of Civil Engineering, Stanford University, Stanford, USA, 1999. [Google Scholar] [Publisher Link]

[26] ASCE, *Minimum Design Loads for Buildings and Other Structures*, American Society of Civil Engineers, Reston, USA, 2016.

[27] AISC, "*ANSI/AISC 360-16, Specification for Structural Steel Buildings*," American Institute of Steel Construction Inc, Chicago, IL, USA, 2016. [Publisher Link]

[28] ICC, *International Building Code*, International Code Council, Whittier, USA, 2006. [Google Scholar] [Publisher Link]

[29] CSI, *SAP2000: Integrated Software for Structural Analysis and Design*, Version 18.2, Computers and Structures Inc, Berkeley, CA, USA, 2016. [Publisher Link]

[30] ATC, *ATC-40 Seismic Evaluation and Retrofit of Concrete Buildings*, Applied Technology Council, Redwood, California, USA, 1996. [Google Scholar] [Publisher Link]

[31] FEMA, FEMA 356: Pre-Standard and Commentary for the Seismic Rehabilitation of Buildings, Federal Emergency Management Agency, Washington, DC, USA, 2000. [Google Scholar] [Publisher Link]

[32] Avtar Pall, and R. Tina Pall, "Performance-Based Design using Pall Friction Dampers - An Economical Design Solution," *13th World Conference on Earthquake Engineering*, Vancouver, B.C., Canada, 2004. [Google Scholar] [Publisher Link]

[33] P. Baktash, and C. Marsh, "Seismic Behavior of Friction Damped Braced Frames," *3rd US National Conference on Earthquake Engineering*, Charleston, SC, USA, 1986. [Google Scholar]

[34] ASCE, *SEI/ASCE 41-06, Seismic Rehabilitation of Existing Buildings*, American Society of Civil Engineers, Reston, USA, 2006. [Publisher Link]

[35] Dimitrios Vamvatsikos, and C. Allin Cornell,, "Applied Incremental Dynamic Analysis," *Earthquake Spectra*, vol. 20, no. 2, pp. 523-553, 2004. [CrossRef] [Google Scholar] [Publisher Link]

[36] Vishal Bhatia, and Siddhartha Ghosh, "Seismic Upgrading of Non-Ductile Steel Frames Using Steel Plate Shear Walls," *International Journal of Advanced Structural Engineering*, vol. 2, no.2, pp. 115-131, 2011. [Google Scholar] [Publisher Link]

[37] Farzad Mirzaie Aminian, Ehsan Khojastehfar, and Hamid Ghanbari, "Effects of Near-Fault Strong Ground Motions on Probabilistic Structural Seismic-Induced Damages Seismic Rehabilitation of Existing Buildings," *Civil Engineering Journal*, vol. 5, no.4, pp. 796-809, 2019. [CrossRef] [Google Scholar] [Publisher Link]

[38] Keith Porter, Robert Kennedy, and Robert Bachman,, "Creating Fragility Functions for Performance-Based Earthquake Engineering," *Earthquake Spectra*, vol. 23, no.2, pp. 471-489, 2007. [CrossRef] [Google Scholar] [Publisher Link]

[39] Jack W. Baker, "Efficient Analytical Fragility Function Fitting Using Dynamic Structural Analysis," *Earthquake Spectra*, vol. 31, no. 1, pp. 579-599, 2015. [CrossRef] [Google Scholar] [Publisher Link]